Japan Bilingual Publishing Co.

New Environmentally-Friendly Materials

https://ojs.bilpub.com/index.php/nefm

ARTICLE

Ag Nanoparticles Obtained by Green Synthesis as Bactericidal Agents in Water-Based Paints

Sandra Gabriela Gómez de Saravia [1,2*] , ***Silvia Elena Rastelli*** [1,3] , ***Erasmo Gámez-Espinosa*** [1,4] , ***Natalia Bellotti*** [1,3] , ***Cecilia Deyá*** [1,5] , ***Marisa Viera*** [1,5]

[1] *Centro de Investigación y Desarrollo en Tecnología de Pinturas y Recubrimientos, La Plata 1900, Argentina*

[2] *Instituto de Ciencias de la Salud, Universidad Nacional Arturo Jauretche, Florencio Varela 1888, Argentina*

[3] *Facultad de Ciencias Naturales, Universidad Nacional de La Plata, La Plata 1900, Argentina*

[4] *Facultad de Ciencias Exactas, Universidad Nacional de La Plata, La Plata 1900, Argentina*

[5] *Facultad de Ingeniería, Universidad Nacional de La Plata, La Plata 1900, Argentina*

ABSTRACT

To control the proliferation of microorganisms and its associated risks, protective surface coatings are being developed. Among the most promising solutions is the incorporation of silver nanoparticles (AgNPs) into paint formulations. Traditional physical and chemical nanoparticles synthesis pose health and environmental risks. The concept of "green nanoparticles" refers to the synthesis of nanoparticles using environmentally benign routes. The aim of this work was to obtain silver nanoparticles (AgNPs) using a green synthesis technique, incorporate them into a polymeric coating, and evaluate their effectiveness as a potential hygienic paint against both gram-positive and gram-negative bacteria. AgNPs were obtained by adding *Schinopsis balansae* (TS) or *Caesalpinia spinosa* (TC) tannin solution to an aqueous solution of $AgNO_3$. The AgNPs were characterized by UV-Visible spectroscopy, Fourier-transform infrared spectroscopy (FTIR), transmission electron microscopy, scanning electron microscopy, and energy-dispersive X-Ray spectroscopy. A polymeric coating was formulated with nanoparticles. To evaluate the antibacterial

*CORRESPONDING AUTHOR:
Sandra Gabriela Gómez de Saravia, Centro de Investigación y Desarrollo en Tecnología de Pinturas y Recubrimientos, La Plata 1900, Argentina; Instituto de Ciencias de la Salud, Universidad Nacional Arturo Jauretche, Florencio Varela 1888, Argentina; Email: s.gomez@cidepint.ing.unlp.edu.ar

ARTICLE INFO
Received: 14 March 2026 | Revised: 18 April 2026 | Accepted: 26 April 2026 | Published Online: 3 May 2026
DOI: https://doi.org/10.55121/nefm.v5i1.1265

CITATION
de Saravia, S.G.G., Rastelli, S.E., Gámez-Espinosa, E., et al., 2026. Ag Nanoparticles Obtained by Green Synthesis as Bactericidal Agents in Water-Based Paints. New Environmentally-Friendly Materials. 5(1): 40–51. DOI: https://doi.org/10.55121/nefm.v5i1.1265

coating efficiency, the modified ISO 22196 method was applied. The concentration and origin of tannin are factors that influence the size and polydispersity of the NPs; TS-AgNPs exhibited higher polydispersity than TC-AgNPs. Coatings incorporating TC-AgNPs exhibited the highest antibacterial efficacy, inhibiting all bacterial strains except *Bacillus cereus*. These results support the feasibility of integrating eco-friendly AgNPs into polymeric coatings for biodeterioration control in indoor environments.

Keywords: Environmentally Friendly Synthesis; Silver Nanoparticles; Antibacterial Activity; Coatings; Biodeterioration; Hygienic Paint

1. Introduction

Building materials can serve as substrates for a range of microorganisms, including algae, bacteria, and fungi. Their growth promotes biofilm formation, which traps dust and other particles, leading to undesirable aesthetic changes and, in many cases, to the biodeterioration of the materials [1,2]. Moreover, the proliferation of biodeteriorating microorganisms can affect indoor air quality, posing health risks to occupants and increasing the incidence of respiratory illnesses. Airborne bacteria, for example, can easily colonize surfaces, especially in densely populated or poorly ventilated environments [3]. *Bacillus* spp. are known for producing food poisoning toxins, and forming resistant spores that are readily dispersed through the air [4]. *Staphylococcus aureus*, commonly associated with skin infections and respiratory diseases, spreads via respiratory droplets in crowded spaces [5]. While *Escherichia coli* is typically found in the intestinal tract, the pathogenic strains can cause severe illness and may be airborne in cases of fecal contamination [6]. Another example is *Pseudomonas aeruginosa*, an opportunistic pathogen known for its antibiotic resistance, which can be found in hospital air systems, particularly those with centralized ventilation [7].

To control the proliferation of these microorganisms, and its associated risks, protective surface coatings are being developed. Among the most promising solutions is the incorporation of silver nanoparticles (AgNPs) into paint formulations. These nanoparticles help preserve the structural integrity of materials while offering long-lasting antimicrobial protection [8]. Due to their distinctive physicochemical properties, nanoparticles (NPs) are capable of interacting with attached microorganisms on a wide range of materials, such as mortar, wood, metals, and painted surfaces, exerting inhibitory effects on microbial growth and biofilm formation [9].

Although physical and chemical methods, such as laser ablation, sol-gel processes, and electro-explosion, are commonly used to synthesize NPs, some of them can entail environmental and health hazards [10,11]. Physical techniques generally require substantial energy, space, and time while offering low yields. Chemical methods, on the other hand, typically involve toxic reducing and stabilizing agents, making them unsuitable for biological applications [12]. NPs have broad applications in medicine and agriculture [13,14] making it crucial to adopt safer manufacturing methods. "Green synthesis" is based on chemical methodologies and processes that can benefit chemical synthesis in terms of energy efficiency, conservation of resources, product selectivity, operational simplicity, health, safety, and environmental impact [11]. For this reason, it offers an environmentally friendly alternative for producing NPs. This approach utilizes extracts from plants, algae, and bacteria, which contain proteins and other biological substances that act as reducing agents, enabling the synthesis and stabilization of NPs without the use of hazardous chemicals [15–19]. AgNPs have antibacterial properties [20–22], although their efficacy can vary depending on the bacterial strain [23].

Recently, the antimicrobial activity against filamentous fungi of AgNPs obtained in *Schinopsis balansae* and *Caesalpinia spinosa* tannin solutions, along with their internalization in protective coatings, was reported [24]. Considering the environmental advantages of green synthesis, particularly in reducing the ecological footprint of manufacturing processes, the aim of this work was to obtain AgNPs using a green synthesis technique, incorporate them into a polymeric coating, and evaluate their effectiveness as a potential hygienic paint against both gram-positive and gram-negative bacteria.

2. Materials and Methods

2.1. Green Synthesis and Characterization of Nanoparticles

Commercial tannins from two native species, *Shinopsis balansae* Engl. and *Caesalpinia spinosa* (Molina) Kuntze, were used to carry out the green synthesis of nanoparticles. The geographic distribution of the genus *Schinopsis* (Anacardiaceae) is restricted to the so-called tropical seasonal dry forests and the subtropical Chaco forests of South America (endemic to the Humid Chaco of north-central Argentina, central Paraguay, and small portions of southwestern Brazil, as well as southeast of Bolivia) [25]. *Caesalpinia spinosa* (Caesalpinaceae) is a species native to Peru, widely distributed in Venezuela, Colombia, Ecuador, Peru, Bolivia, and the north of Chile, growing wild or cultivated in several of these countries [26]. AgNPs solutions of 500 mg L^{-1} were obtained by adding commercial tannin of *Schinopsis balansae* (UNITAN, Argentina) or *Caesalpinia spinosa* (INDUNOR, Argentina) to an aqueous solution of $AgNO_3$ (final concentration 10^{-2} M), stirred for 30 min at 60 ℃; pH was adjusted to 7 employing NH_4OH solution after the tannin solution addition. The formation of AgNPs was initially evidenced by a characteristic color change of the solution. The nanoparticles were obtained as stable colloidal suspensions and were used directly without further purification steps such as centrifugation, washing, or filtration, as the tannin components act as both reducing and stabilizing agents. The particles in suspension were kept at 4 ℃ in amber flasks [24].

Subsequently, the AgNPs were characterized by UV-Visible (UV-Vis) and Fourier Transform Infrared (FTIR) spectroscopies and observed by transmission electron microscopy (TEM) and scanning electron microscopy (SEM) with coupled energy-dispersive X-ray spectroscopy (EDS). The absorbance measurements of UV-Vis spectra were made in a UV-2600 240V EN spectrophotometer to verify the presence and stability of the NPs in suspension after 24 h. FTIR spectroscopy was performed on the purified nanoparticles using the KBr disk method with a PerkinElmer Spectrum One spectrometer. TEM (Zeiss EM 109T) operated at an acceleration voltage of 80 kV and equipped with a digital camera (Gatan ES1000W) was applied to confirm the obtaining of the NPs, observe their morphology, and size. The NPs were purified by successive washes using a microcentrifuge (DLAB D3024R) at 15,000 rpm for 20 min at 20 ℃ to be observed by SEM. The SEM observations (Philips FEI Quanta 200) were made at low vacuum (10^{-2} torr).

2.2. Microorganisms Used for Assays

For antibacterial assays, reference gram-positive bacteria, such as *Bacillus cereus* ATCC 10876 and *Staphylococcus aureus,* and gram-negative bacteria, such as *Escherichia coli* ATCC 11229 and *Pseudomonas aeruginosa* PAO 1, maintained in nutrient agar slants in our laboratory, were used.

2.3. Preliminary Diffusion Tests for Bacteria

The antibacterial activity of TS and TC solutions, and TS-AgNPs and TC-AgNPs, was assessed using the agar diffusion method, commonly known as the Kirby-Bauer method. Bacterial inocula with an $OD_{(600\ nm)} \approx 0.1$ ($\approx 10^8$ CFU ml^{-1}) were prepared in Muller-Hinton (M-H) broth (Britania, Argentina), from fresh 24 h agar slant cultures. M-H agar plates were inoculated by swab in three directions, except for *S. aureus*, which was seeded by spreading 200 µl of the inoculum with a Drigalsky spatula. Sterile filter paper disks of 6 mm diameter were placed in the plates. Eight µl of TS and TC solutions, TS-AgNPs, TC-AgNPs (both at a concentration of 1 mg ml^{-1}), distilled water (DW) as a negative control, and streptomycin (Sigma-Aldrich, USA), as positive control at 40 mg ml^{-1} were placed on the paper disks. The plates were incubated 18–20 h at 30 ± 2 ℃ and the inhibition growth zones were measured. The assay was performed in triplicate.

2.4. Paint Formulation, Manufacturing, and Characterization

The control paint was prepared in a high-speed disperser with the following composition: 42.09% acrylic resin (1:1, Thyosil E190, Diransa, Argentine), 12.42% TiO_2 (Zamudio, Argentine), 27.32% natural $CaCO_3$ (Cema, Argentine), 2.43% precipitated $CaCO_3$ (FGH, Argentine), 1.97% additives (antifoaming, cellulosic thick-

ener, dispersants, surfactants, coalescents), and 13.77% distilled water (DW) (% by weight). A second paint was prepared by adding to the control paint 0.05% (recommended by the provider) of a commercial biocide based on AgCl (commercial biocide paint). The paints containing AgNPs were prepared by replacing the distilled water in the control paint with the corresponding nanoparticle suspensions (treatment paints: TS-AgNPs paint and TC-AgNPs paint). The final AgNPs concentration in these paints was approximately 0.15 mg/g, calculated from the initial $AgNO_3$ concentration (10^{-2} M).

Paints were characterized by set-to-touch and dry-through times [27], hiding power (by reflectometry employing a BYK Gardner spectro-Guide sphere gloss) and washability test [28].

2.5. Bactericidal Paint Test

To assess the efficiency of the antibacterial paints, the modified ISO 22196 method [29] was employed. Samples of square glasses (25 mm on a side) were painted with the control paint, the commercial biocide paint, and with TS-NPs paint or TC-NPs paint. Two coats of paint were applied with a brush with a difference of 24 h and in perpendicular directions. The painted samples were left to dry for 15 days at room temperature and humidity, then they were sterilized in UV radiation (40 min on each side). The samples were placed (in triplicate) in sterile Petri dishes and inoculated with 0.1 mL of a suspension of the following bacterial strains: *S. aureus* (1.6×10^5 CFU ml^{-1}), *B. cereus* (3×10^4 CFU ml^{-1}), *E. coli* (1×10^5 CFU ml^{-1}) and *P. aeruginosa* (6×10^4 CFU ml^{-1}). Each sample was covered with a sterilized polyethylene film, and the Petri dishes were incubated 24 h at 30 ºC (±2 ºC). After this time, the film was removed, the samples were imprinted 3 times in a new Petri dish with plate count agar and incubated 24 h at 30 ºC (±2 ºC). The antibacterial efficiency was evaluated on a scale from 0 to 5 based on the extent of bacterial growth [30,31] as follows: 0 = without growth; 1 = detectable amount (single colony); 2 = detectable amount (combined colony); 3 = second imprint, distinguishable colonies, third imprint can be detected; 4 = third imprint, distinguishable colonies; 5 = overgrown, continuous growth.

2.6. Statistical Analysis

Statistical analysis was performed using RStudio software (version 2026.04.0 Build 526). A one-way ANOVA was conducted to assess significant differences in the inhibition growth zone among the various antimicrobial compounds using the multcomp package. This analysis identified whether there were statistically significant differences between the paints. When significant differences were detected, a post-hoc Tukey HSD test was applied to determine which pairs of compounds exhibited specific differences. In addition, antibacterial activity based on ordinal scores (0–5) was analyzed using the Kruskal–Wallis test (R, stats package) to evaluate differences among paint formulations for each microorganism. Data processing was performed using the dplyr and tidyr packages. Results were considered statistically significant at $p \leq 0.05$.

3. Results and Discussion

3.1. Green Synthesis and Characterization of Nanoparticles

AgNPs were successfully synthesized using tannin solutions from *Schinopsis balansae* (TS) and *Caesalpinia spinosa* (TC) as reducing agents in an aqueous $AgNO_3$ solution, resulting in TS-AgNPs and TC-AgNPs, respectively. The formation of AgNPs using tannins is strongly influenced by reaction conditions, particularly temperature and pH. In this study, synthesis was carried out at 60 ºC with pH adjusted to neutral conditions, which favors the activation of phenolic groups involved in the reduction of Ag^+ ions. Temperature also enhances reaction kinetics and nucleation processes. In previous studies, other conditions (temperature and pH) were evaluated for the green synthesis of AgNPs [32,33]. Although nanoparticle formation was observed over a range of conditions, the synthesis performed at 60 ºC and pH = 7 was found to be more efficient, producing stable Ag NPs. **Figure 1a** shows the UV–vis spectra of AgNPs synthesized with *S. balansae* and *C. spinosa* tannin after 24 h. Bands between 400 and 450 nm, corresponding to the surface plasmon band of AgNPs, can be observed in both cases, with a signal around 410 nm. The positioning of wavelengths is predominantly influenced by factors such as dimensions, morphology, and the particle size distribution [34].

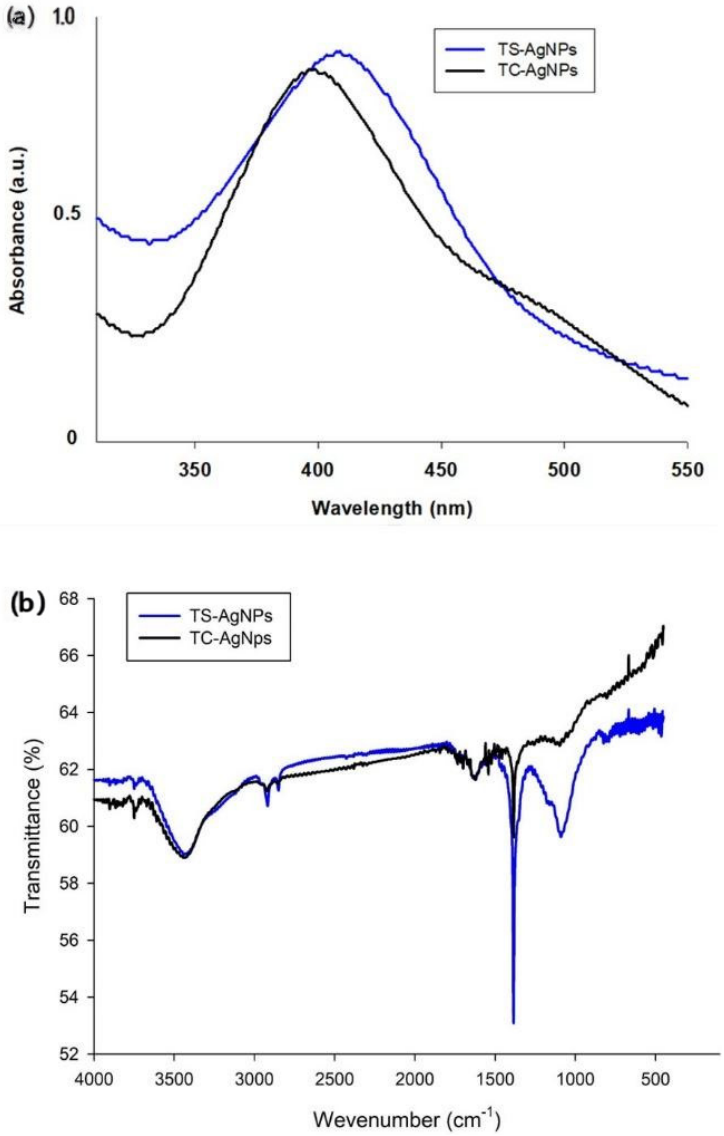

Figure 1. (**a**) UV–Vis; (**b**) FTIR spectra of AgNPs synthesized with *S. balansae* (TS-AgNPs) and *C. spinosa* (TC-AgNPs) tannin after 24 h.

In addition, the FTIR spectra shown in **Figure 1b** provide further insights into the nanoparticle synthesis mechanism. The FTIR spectroscopic analysis of AgNPs synthesized using TS and TC reveals characteristic signals that confirm the involvement of polyphenols in both the reduction and stabilization processes. Both spectra exhibit a broad band in the 3,200–3,400 cm^{-1} region, attributed to the stretching vibration of hydroxyl (−OH) groups, typical of phenolic compounds. Additional bands are observed around 1600–1400 cm^{-1}, associated with C=C vibrations of the aromatic ring and stretching of conjugated carbonyl (C=O) groups, suggesting the presence of gallic or ellagic acid-type structures, which are predominant in these tannins. The pronounced intensity of the signals in TS-AgNPs, particularly near 1,380 cm^{-1} and 1,040 cm^{-1}, suggests a stronger interaction of phenolic functional groups with the nanoparticle surface, enhancing both the reduction of silver ions (Ag^{+}) and the colloidal stabilization of the resulting material. These findings highlight the dual role of polyphenols as reducing and capping agents in the green synthesis of AgNPs.

The TEM images of TS-AgNP and TC-AgNP are shown in **Figure 2**. Both are almost spherical in shape, with average sizes of 11 nm (*sd* = 4) and 14 nm (*sd* = 2), respectively. This is consistent with the UV-Vis spectra, as small spherical AgNPs exhibit an extended surface plasmon reso-

nance band in the range of 350–500 nm [34]. The concentration and origin of tannin are factors that influence the size and polydispersity of the NPs [35]. TS-AgNPs (**Figure 2a**) exhibited higher polydispersity than TC-AgNPs (**Figure 2b**), possibly due to their derivation from different tannins, despite both tannins being used at the same concentration (500 mg L^{-1}). Additionally, both particles displayed the same morphology, possibly because they were phytosynthesized under identical conditions of biochemical reducing agents (polyphenols) concentration and temperature.

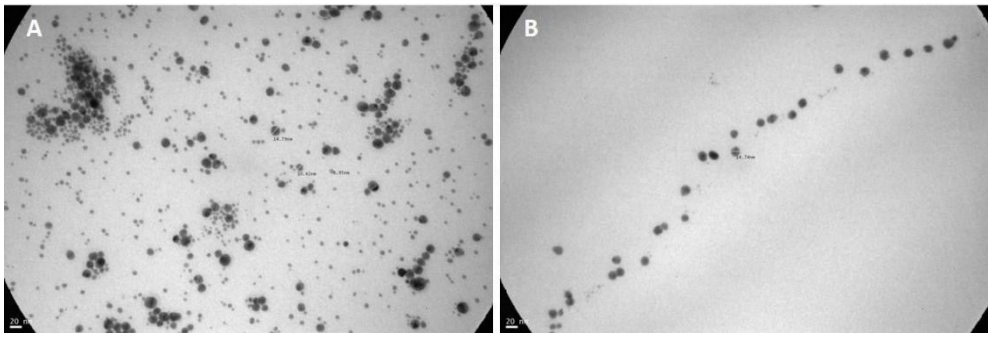

Figure 2. TEM images (250,000×) of AgNPs synthesized with TS and TC tannin solution: (**a**) TS-AgNPs; (**b**) TC-AgNPs.
Note: Scale bar in each micrograph: 20 nm.

SEM micrographs and EDS spectra of AgNPs are depicted in **Figure 3**. SEM images of TS-AgNPs (**Figure 3a**) and TC-AgNPs (**Figure 3b**) revealed a tightly packed arrangement of particles. This clustering of nanoparticles is expected, as nanoparticles of metals have high surface energy and they tend to clump [36]. EDS spectra of TS-AgNPs (**Figure 3c**) and TC-AgNPs (**Figure 3d**) exhibited a distinct peak corresponding to Ag at 3 keV, providing clear confirmation of the presence of this metal in the obtained nanoparticles. This finding further validates the results obtained from other particle characterization techniques described above (UV–Vis spectroscopy and TEM images).

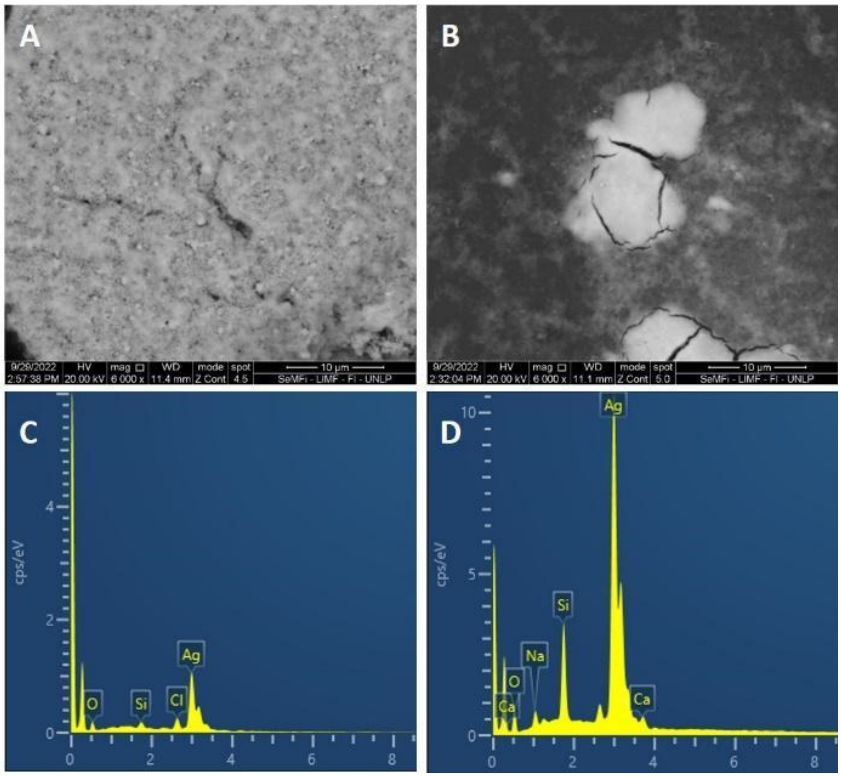

Figure 3. SEM micrographs (6,000×) of (**a**) TS-AgNPs ; (**b**) TC-AgNPs; EDS spectra of (**c**) TS-AgNPs; (**d**) TC-AgNPs.
Note: Scale bar in each micrograph: 10 µm.

3.2. Diffusion Tests for Bacteria

The antibacterial activity determined using the disk diffusion method is shown in **Figure 4**. As can be seen, TC and TS exhibited no bactericidal activity against any of the tested bacterial strains (inhibition zone = 6 ± 0 mm), which was comparable to the negative control with distilled water (DW). In contrast, all bacterial strains showed some degree of growth inhibition when exposed to TC-AgNPs and TS-AgNPs. *P. aeruginosa* was the most susceptible strain (TC-AgNPs = 16 ± 1 mm, TS-AgNPs = 17 ± 2 mm). The one-way ANOVA revealed statistically significant differences in the inhibition zones among the different compounds ($F = 76.05$, $p < 0.001$). The Tukey HSD test results showed that streptomycin had a significantly greater effect on bacterial growth inhibition compared to all other compounds ($p < 0.001$). This finding is consistent with the clinical use of streptomycin as an effective antibiotic against a wide range of bacteria. The difference in behavior can be attributed to the greater diffusion of the antibiotic compared to the nanoparticles [37,38]. Furthermore, no significant differences were observed between TC-AgNPs and TS-AgNPs in terms of inhibition zones ($p = 0.993$). This lack of significant difference suggests that the antimicrobial activity of these formulations could be primarily attributed to the AgNPs, whose efficacy appears unaffected by the specific tannin matrix in which they are synthesized, especially considering that the tannins alone, as demonstrated by the test, did not exhibit antimicrobial activity.

This finding could have practical implications for the design of antimicrobial coatings, suggesting that the choice of tannin source can be based on factors such as availability, cost, or additional properties, without compromising the antimicrobial efficacy provided by the AgNPs. Regardless of this, the results are favorable given that the goal of these nanomaterials is their incorporation and long-term retention into paint matrices throughout the service life of the coating.

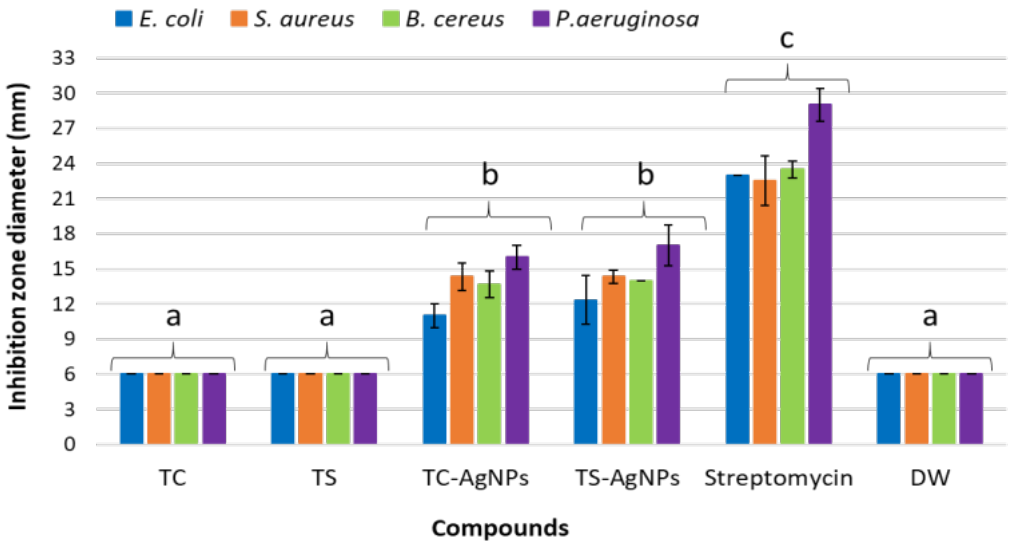

Figure 4. Antibacterial activity of tannin solutions (TC, TS), nanoparticles (TC-AgNPs, TS-AgNPs), positive (Streptomycin), and negative (DW = distilled water) controls.

Note: Different letters correspond to statistically significant differences for the Tukey HSD test ($p < 0.05$, n = 3).

3.3. Paint Characterization

The results of the characterization tests conducted on the paints are shown in **Table 1**. The addition of biocides slightly enhances the hiding power of the paints, while drying times are shortened when AgNPs are added. Washability was satisfactory in all cases, as evidenced by the wet scrub resistance, which met the 1,500 cycles requirement established by IRAM 1077 [28] for outdoor paints after 21 days of conditioning.

Table 1. Characterization of samples through hiding power, drying times, and washability tests.

Paints	Hiding Power (%)	Set to Touch Time (min)	Hard Dry Time (min)	Washability (Cycles)
Control	89.9	120	140	1,500
Commercial biocide	99.3	120	140	1,500
TS-AgNPs	99.9	80	110	1,500
TC-AgNPs	100.0	90	110	1,500

3.4. Antibacterial Activity of Paints

Silver nanoparticles obtained by green synthesis of different plants and biological organisms exhibit antibacterial activity. Nanoparticles cause interference in DNA, which leads to the inhibition of respiratory enzymes and the suppression of the electron transport chain, losing DNA's ability to replicate [19]. AgNPs exhibit antibacterial activity because of their high surface-to-volume ratio, which enhances the interaction, and improves biocidal effectiveness. Silver's antimicrobial action is strongly based on the Ag^+ ion that prevents the growth of bacteria [17]. The phospholipids and proteins present in the bacterial cell membrane give it a negative charge. When Ag^+ ions come into contact with a bacterial wall, they adhere to the bacteria and damage the bacterial structure [19,39,40]. Silver has relatively lower antimicrobial effects on gram-positive bacteria than on gram-negative bacteria. The results obtained for the resistance test according to the modified ISO 22196 standard are shown in **Figure 5**. As expected, the growth of all bacterial strains tested on the control paint was observed. Unexpectedly, this also happened on the paint with the commercial biocide based on silver chloride. The TS-AgNPs paint, exerting total inhibition on the *S. aureus* growth, and only slightly decreasing on the *E. coli* growth. The highest antibacterial activity was exerted by the TC-AgNPs paint, for which only slight variations in *B. cereus* growth were observed among the evaluated paints, while the growth of all other bacterial strains was inhibited. Significant differences in antibacterial activity among the evaluated paints were observed for *E. coli* (Kruskal–Wallis, $p = 0.0151$), *S. aureus* ($p = 0.0117$) and *P. aeruginosa* ($p = 0.0117$). These results indicate that antibacterial performance varied among paint formulations. In contrast, no significant differences were detected for *B. cereus* ($p = 0.3199$), indicating similar behavior among the tested paints. These results agree with the characteristics of the AgNPs synthesized from each tannin solution. As observed in **Figure 2**, the size of the TC-NPs is greater than the TS-NPs, however, TS-NPs presents a greater variation in size ($sd = 4$) and greater agglomeration of the NPs, which makes it difficult for them to penetrate inside the cell, modifying its bactericidal effect. Consequently, TS-AgNPs and TC-AgNPs, effectively internalized in TS-AgNPs and TC-AgNPs respective paints, could potentially damage respiratory enzymes by generating reactive oxygen species, and could cause cell lysis, cytoplasm leakage, and bacterial death by extracting electrons from membranes of the gram-negative and gram-positive bacteria selected for this paper.

These results are novel as they constitute the first report of the antibacterial activity of nanomaterial-functionalized paints obtained from tannins of *Schinopsis balansae* and *Caesalpinia spinosa*. However, it is advisable to study the release of the particles in the coating and evaluate their antimicrobial activity after an accelerated aging test. The absence of accelerated aging evaluation represents a limitation of this study. The evaluation of Ag^+ release and leaching kinetics from the paint matrix was beyond the scope of this study; although antimicrobial activity was confirmed over a 30-day period, additional investigations are needed to better understand the release behavior of silver species and the long-term performance of these coatings under service conditions. To ensure these formulations do not lead to secondary pollution, ecotoxicological studies are recommended to assess the long-term environmental impact of AgNPs, particularly in soil and aquatic systems, striking a balance between antimicrobial efficacy and environmental sustainability. This research explores the application of environmentally friendly nanotechnology in mitigating microbial contamination in indoor environments, thereby contributing to improved indoor air quality and public health.

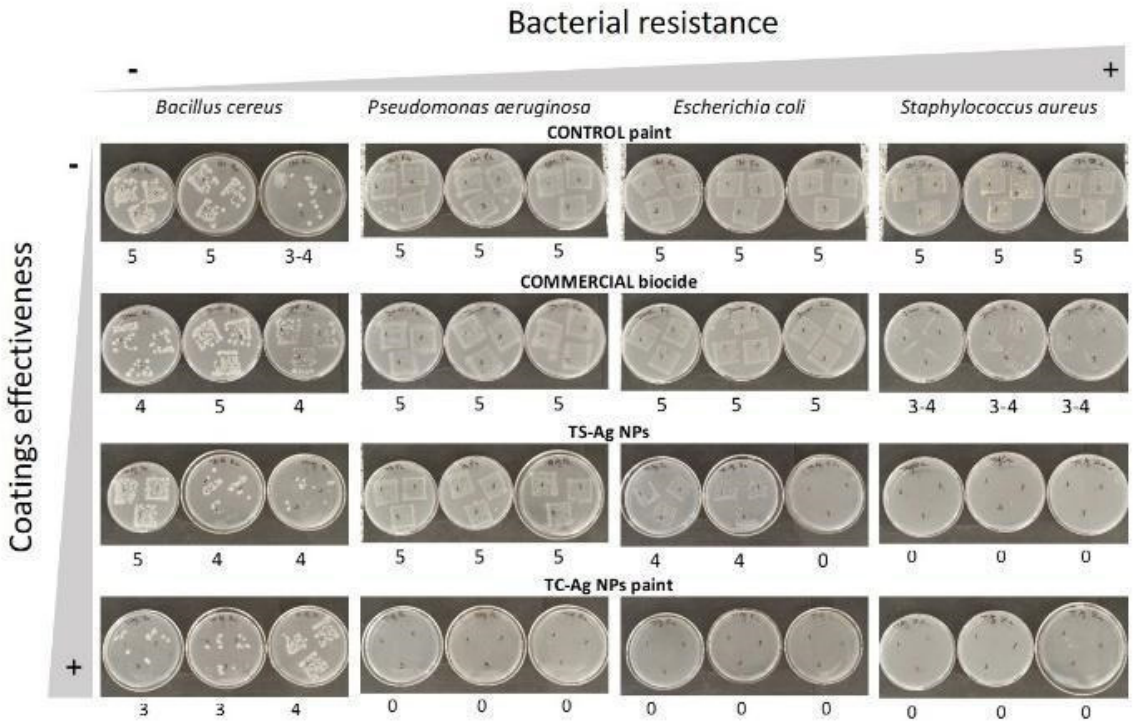

Figure 5. Antibacterial activity of paints on assayed bacteria.

Note: Scale values: 0 = without growth; 1 = detectable amount (single colony); 2 = detectable amount (combined colony); 3 = second imprint, distinguishable colonies, third imprint can be detected; 4 = third imprint, distinguishable colonies; 5 = overgrown, continuous growth.

4. Conclusions

The characteristics of silver nanoparticles varied according to the tannin solution used for green synthesis. Coatings incorporating TC-AgNPs exhibited the highest antibacterial efficacy, inhibiting all bacterial strains except *Bacillus cereus*. TS-AgNPs coatings completely inhibited *Staphylococcus aureus* and moderately reduced *Escherichia coli.* These results support the feasibility of integrating eco-friendly AgNPs into polymeric coatings for biodeterioration control in indoor environments.

Author Contributions

Conceptualization, S.G.G.d.S., S.E.R., E.G.-E., N.B., C.D. and M.V.; methodology, S.G.G.d.S., S.E.R., E.G.-E., N.B., C.D. and M.V.; investigation, S.E.R. and E.G.-E.; resources, S.G.G.d.S.; writing—original draft preparation, S.E.R., E.G.-E. and C.D.; writing—review and editing, S.G.G.d.S. and S.E.R.; supervision, S.G.G.d.S., N.B., C.D. and M.V.; project administration, S.G.G.d.S.; funding acquisition, S.G.G.d.S. All authors have read and agreed to the published version of the manuscript.

Funding

This work was supported by grants Res. 1517/20 and Res. 389/21 from the Commission of the Province of Buenos Aires, and National University of La Plata 11/I238.

Institutional Review Board Statement

Not applicable.

Informed Consent Statement

Not applicable.

Data Availability Statement

Not applicable.

Conflicts of Interest

The authors declare no conflict of interest.

AI Use Statement

The authors declare that no artificial intelligence (AI) tools were used in the preparation of this manuscript.

References

[1] Becerra, J., Zaderenko, A.P., Sayagués, M.J., et al., 2018. Synergy achieved in silver-TiO2 nanocomposites for the inhibition of biofouling on limestone. Building and Environment. 141, 80–90. DOI: https://doi.org/10.1016/j.buildenv.2018.05.020

[2] Nowicka-Krawczyk, P., Komar, M., Gutarowska, B., 2022. Towards understanding the link between the deterioration of building materials and the nature of aerophytic green algae. Science of The Total Environment. 802, 149856. DOI: https://doi.org/10.1016/j.scitotenv.2021.149856

[3] Carrazana, E., Ruiz-Gil, T., Fujiyoshi, S., et al., 2023. Potential airborne human pathogens: A relevant inhabitant in built environments but not considered in indoor air quality standards. Science of The Total Environment. 901, 165879. DOI: https://doi.org/10.1016/j.scitotenv.2023.165879

[4] Tang, C.-S., Wan, G.-H., 2013. Air Quality Monitoring of the Post-Operative Recovery Room and Locations Surrounding Operating Theaters in a Medical Center in Taiwan. PLoS ONE. 8(4), e61093. DOI: https://doi.org/10.1371/journal.pone.0061093

[5] Madsen, A.M., Moslehi-Jenabian, S., Islam, M.Z., et al., 2018. Concentrations of Staphylococcus species in indoor air as associated with other bacteria, season, relative humidity, air change rate, and *S. aureus*-positive occupants. Environmental Research. 160, 282–291. DOI: https://doi.org/10.1016/j.envres.2017.10.001

[6] Kaper, J.B., Nataro, J.P., Mobley, H.L.T., 2004. Pathogenic *Escherichia coli*. Nature Reviews Microbiology. 2(2), 123–140. DOI: https://doi.org/10.1038/nrmicro818

[7] Lyczak, J.B., Cannon, C.L., Pier, G.B., 2000. Establishment of infection: Lessons from a versatile opportunist. Microbes and Infection. 2(9), 1051–1060. DOI: https://doi.org/10.1016/S1286-4579(00)01259-4

[8] Ganguli, P., Chaudhuri, S., 2021. Nanomaterials in antimicrobial paints and coatings to prevent biodegradation of man-made surfaces: A review. Materials Today: Proceedings. 45, 3769–3777. DOI: https://doi.org/10.1016/j.matpr.2021.01.275

[9] Li, Q., Mahendra, S., Lyon, D.Y., et al., 2008. Antimicrobial nanomaterials for water disinfection and microbial control: Potential applications and implications. Water Research. 42(18), 4591–4602. DOI: https://doi.org/10.1016/j.watres.2008.08.015

[10] Bloch, K., Pardesi, K., Satriano, C., et al., 2021. Bacteriogenic Platinum Nanoparticles for Application in Nanomedicine. Frontiers in Chemistry. 9, 624344. DOI: https://doi.org/10.3389/fchem.2021.624344

[11] Nandihalli, N., Gregory, D.H., Mori, T., 2022. Energy-Saving Pathways for Thermoelectric Nanomaterial Synthesis: Hydrothermal/Solvothermal, Microwave-Assisted, Solution-Based, and Powder Processing. Advanced Science. 9(25), 2106052. DOI: https://doi.org/10.1002/advs.202106052

[12] Siddiqi, K.S., Husen, A., Rao, R.A.K., 2018. A review on biosynthesis of silver nanoparticles and their biocidal properties. Journal of Nanobiotechnology. 16(1), 14. DOI: https://doi.org/10.1186/s12951-018-0334-5

[13] Elbagory, A.M., Ekpo, O.E., 2025. Middle Eastern plants as a source of bioactive metal nanoparticles: A critical review. Green Chemistry Letters and Reviews. 18(1), 2507288. DOI: https://doi.org/10.1080/17518253.2025.2507288

[14] Castillo-Henríquez, L., Alfaro-Aguilar, K., Ugalde-Álvarez, J., et al., 2020. Green Synthesis of Gold and Silver Nanoparticles from Plant Extracts and Their Possible Applications as Antimicrobial Agents in the Agricultural Area. Nanomaterials. 10(9), 1763. DOI: https://doi.org/10.3390/nano10091763

[15] Ghosh, S., Gurav, S.P., Harke, A.N., et al., 2016. Dioscorea oppositifolia Mediated Synthesis of Gold and Silver Nanoparticles with Catalytic Activity. Journal of Nanomedicine & Nanotechnology. 7(5). DOI: https://doi.org/10.4172/2157-7439.1000398

[16] Jamdade, D.A., Rajpali, D., Joshi, K.A., et al., 2019. *Gnidia glauca* - and *Plumbago zeylanica* -Mediated Synthesis of Novel Copper Nanoparticles as Promising Antidiabetic Agents. Advances in Pharmacological Sciences. 2019, 1–11. DOI: https://doi.org/10.1155/2019/9080279

[17] Ghatti, V., Chapi, S., Kumar Kumarswamy, Y., et al., 2025. Strontium-Decorated Ag2O Nanoparticles Obtained via Green Synthesis/Polyvinyl Alcohol Films for Wound Dressing Applications. Materials. 18(15), 3568. DOI: https://doi.org/10.3390/ma18153568

[18] Pattadakal, S., Ghatti, V., Chapi, S., et al., 2025. Poly(vinyl alcohol) Nanocomposites Reinforced with CuO Nanoparticles Extracted by Ocimum sanctum: Evaluation of Wound-Healing Applications. Polymers. 17(3), 400. DOI: https://doi.org/10.3390/

polym17030400

[19] Mikhailova, E.O., 2024. Green Silver Nanoparticles: An Antibacterial Mechanism. Antibiotics. 14(1), 5. DOI: https://doi.org/10.3390/antibiotics14010005

[20] Lara, H.H., Ayala-Núñez, N.V., Ixtepan Turrent, L.D.C., et al., 2010. Bactericidal effect of silver nanoparticles against multidrug-resistant bacteria. World Journal of Microbiology and Biotechnology. 26(4), 615–621. DOI: https://doi.org/10.1007/s11274-009-0211-3

[21] Bekhradian, A., Karami, B., Rajabi, H.R., 2024. Green synthesis of silver/silver oxide nanostructures using the Malva sylvestris extract prior to simultaneous distillation extraction: synthesis, phytochemical and biological analysis. Preprint. DOI: https://doi.org/10.21203/rs.3.rs-4861630/v1

[22] Habeeb Rahuman, H.B., Dhandapani, R., Narayanan, S., et al., 2022. Medicinal plants mediated the green synthesis of silver nanoparticles and their biomedical applications. IET Nanobiotechnology. 16(4), 115–144. DOI: https://doi.org/10.1049/nbt2.12078

[23] Yoon, K.-Y., Hoon Byeon, J., Park, J.-H., et al., 2007. Susceptibility constants of *Escherichia coli* and Bacillus subtilis to silver and copper nanoparticles. Science of The Total Environment. 373(2–3), 572–575. DOI: https://doi.org/10.1016/j.scitotenv.2006.11.007

[24] Gámez-Espinosa, E., Deyá, C., Cabello, M., et al., 2023. Control of fungal deterioration of ceramic materials by green nanoadditives-based coatings. Nano-Structures & Nano-Objects. 36, 101069. DOI: https://doi.org/10.1016/j.nanoso.2023.101069

[25] Barberis, I.M., Mogni, V., Oakley, L., et al. 2012. Biology of Southern Species: *Schinopsis balansae* Engl. (Anacardiaceae). Kurtziana. 37(2), 59–86. (in Spanish)

[26] Robledo Restrepo, S.M., Quintero, J., Higuita, J., et al., 2020. *Caesalpinia spinosa* (Molina) Kuntze: A New Promise for the Topical Treatment of Cutaneous Leishmaniasis. Revista de la Academia Colombiana de Ciencias Exactas, Físicas y Naturales. 44(173), 915–936. DOI: https://doi.org/10.18257/raccefyn.1247 (in Spanish)

[27] ASTM International, 2017. ASTM D1640-95: Standard Test Methods for Drying, Curing, or Film Formation of Organic Coatings at Room Temperature. ASTM International: West Conshohocken, PA, USA. Available from: https://store.astm.org/d1640-95r99.html

[28] Instituto Argentino de Normalización y Certificación (IRAM), 2007. IRAM 1109-B15: Paints. General Test Methods. Part B15—Determination of Wet Scrub Resistance. IRAM: Buenos Aires, Argentina. (in Spanish)

[29] International Organization for Standardization (ISO), 2011. ISO 22196:2011—Measurement of Antibacterial Activity on Plastics and Other Non-Porous Surfaces. ISO: Geneva, Switzerland. Available from: https://www.iso.org/standard/54431.html

[30] Habib, S., Lehocky, M., Vesela, D., et al., 2019. Preparation of Progressive Antibacterial LDPE Surface via Active Biomolecule Deposition Approach. Polymers. 11(10), 1704. DOI: https://doi.org/10.3390/polym11101704

[31] Machotová, J., Kalendová, A., Voleská, M., et al., 2020. Waterborne hygienic coatings based on self-crosslinking acrylic latex with embedded inorganic nanoparticles: A comparison of nanostructured ZnO and MgO as antibacterial additives. Progress in Organic Coatings. 147, 105704. DOI: https://doi.org/10.1016/j.porgcoat.2020.105704

[32] Bellotti, N., Romagnoli, R., Quintero, C., et al., 2015. Nanoparticles as antifungal additives for indoor water borne paints. Progress in Organic Coatings. 86, 33–40. DOI: https://doi.org/10.1016/j.porgcoat.2015.03.006

[33] Deyá, C., Bellotti, N., 2017. Biosynthesized silver nanoparticles to control fungal infections in indoor environments. Advances in Natural Sciences: Nanoscience and Nanotechnology. 8(2), 025005. DOI: https://doi.org/10.1088/2043-6254/aa6880

[34] Ider, M., Abderrafi, K., Eddahbi, A., et al., 2017. Silver Metallic Nanoparticles with Surface Plasmon Resonance: Synthesis and Characterizations. Journal of Cluster Science. 28(3), 1051–1069. DOI: https://doi.org/10.1007/s10876-016-1080-1

[35] Guo, J., Wu, H., Liao, X., et al., 2011. Facile Synthesis of Size-Controlled Silver Nanoparticles Using Plant Tannin Grafted Collagen Fiber As Reductant and Stabilizer for Microwave Absorption Application in the Whole Ku Band. The Journal of Physical Chemistry C. 115(48), 23688–23694. DOI: https://doi.org/10.1021/jp207194a

[36] Nandihalli, N., Mori, T., Kleinke, H., 2018. Effect of addition of SiC and Al2O3 refractories on Kapitza resistance of antimonide-telluride. AIP Advances. 8(9), 095009. DOI: https://doi.org/10.1063/1.5034520

[37] Kourmouli, A., Valenti, M., Van Rijn, E., et al., 2018. Can disc diffusion susceptibility tests assess the antimicrobial activity of engineered nanoparticles? Journal of Nanoparticle Research. 20(3), 62. DOI: https://doi.org/10.1007/s11051-018-4152-3

[38] Rosman, N.S.R., Harun, N.A., Idris, I., et al., 2020. Eco-friendly silver nanoparticles (AgNPs) fabricated

by green synthesis using the crude extract of marine polychaete, Marphysa moribidii: Biosynthesis, characterisation, and antibacterial applications. Heliyon. 6(11), e05462. DOI: https://doi.org/10.1016/j.heliyon.2020.e05462

[39] Rajasekharreddy, P., Usha Rani, P., Sreedhar, B., 2010. Qualitative assessment of silver and gold nanoparticle synthesis in various plants: A photobiological approach. Journal of Nanoparticle Research. 12(5), 1711–1721. DOI: https://doi.org/10.1007/s11051-010-9894-5

[40] Kannan, M., Rajarathinam, K., Venkatesan, S., et al., 2017. Silver Iodide Nanoparticles as an Antibiofilm Agent—A Case Study on Gram-Negative Biofilm-Forming Bacteria. In Nanostructures for Antimicrobial Therapy. Elsevier: London, UK. pp. 435–456. DOI: https://doi.org/10.1016/B978-0-323-46152-8.00019-6